[Communication] www.whxb.pku.edu.cn

基于双极性小分子的单层非掺杂红色荧光有机发光二极管

赵云龙 段 炼* 乔 娟 张德强 王立铎 邱 勇
(清华大学化学系, 北京 100084)

摘要: 以双极性小分子 4,9-二(4-(2,2-二苯乙烯基)苯基)萘并[2,3-*c*][1,2,5]噻二唑(BDPNTD)为发光层, 制备得到了单层非掺杂红色荧光有机发光二极管. 通过在阳极 ITO 与有机层 BDPNTD 之间插入 1 nm 厚的 WO_3 或 MoO_3 薄膜, 获得了单层有机发光二极管: 起亮电压为 2.4 V, 最大发光亮度为 4950 cd·m^{-2}, 发光波长为 636 nm, CIE 坐标约为(0.65, 0.35). 这证明了作为修饰层的WO_3或MoO_3薄膜可以改进ITO/BDPNTD界面的空穴注入, 进而在器件中实现空穴与电子的平衡.

关键词: 有机发光二极管; 单层; 非掺杂; 红色荧光; 双极性; ITO 修饰层
中图分类号: O644

Non-doped Single-Layer Red-Emitting Electrofluorescent Devices Based on an Ambipolar Small Molecule

ZHAO Yun-Long DUAN Lian* QIAO Juan ZHANG De-Qiang WANG Li-Duo QIU Yong
(*Department of Chemistry, Tsinghua University, Beijing 100084, P. R. China*)

Abstract: Non-doped red-emitting electrofluorescent single-layer organic light-emitting devices based on an ambipolar small molecule, 4,9-bis(4-(2,2-diphenylvinyl)phenyl)naphtho[2,3-*c*][1,2,5] thiadiazole (BDPNTD), were studied. A WO_3 or MoO_3 buffer layer with an optimized thickness of 1 nm was used and the single-layer device has a low turn-on voltage (2.4 V) and a high luminance (4950 cd·m^{-2}). The maximum emission wavelength was at about 636 nm and the CIE coordinates are at about (0.65, 0.35). We confirmed that the WO_3 or MoO_3 buffer layer can improve hole injection at the ITO/ BDPNTD interface and it creates a hole–electron balance in these devices.

Key Words: Organic light-emitting device; Single-layer; Non-doped; Red-emitting electrofluorescent; Ambipolar; ITO buffer layer

Since Tang and VanSlyke[1] reported efficient electroluminescence of organic materials in 1987, organic light-emitting devices (OLEDs) based on either small molecules or polymers have been intensively studied because of their potential application in flat-panel displays. OLEDs are double-charge injection devices, which require the simultaneous supply of both electrons and holes to the electroluminescent material sandwiched between two electrodes[2]. To meet this demand, two strategies including the fabrication of multilayer devices[3] and integrating hole-transporting, electron-transporting, and light emitting components into a single layer[4–5], have been developed. However, fabrication of multilayer devices is often tedious, difficult, and more expensive than single-layer devices[6]. Generally, single-layer OLEDs can be achieved by two paths: doping dyes into the host material[4] or combining electron and hole transporting chromophores into a single light-emitting molecule[5–10]. Recently, Wu *et al*.[7] reported a compound containing benzimidazole and arylamine units, and the electron and hole mobilities of which are both about 10^{-5} $cm^2 \cdot V^{-1} \cdot s^{-1}$. Moreover, the non-doped device based on this compound emitted blue light with a current efficiency of 2.5 cd·

Received: December 16, 2009; Revised: January 27, 2010; Published on Web: January 29, 2010.
*Corresponding author. Email: duanl@mail.tsinghua.edu.cn; Tel: +86-10-62779988; Fax: +86-10-62795137.
The project was supported by the National Natural Science Foundation of China (50873055) and National Key Basic Research Program of China (2006CB806203).
国家自然科学基金(50873055)和国家重点基础研究发展规划项目(973)(2006CB806203)资助

A^{-1}, which is the best result among other non-doped blue-emitting single-layer OLEDs. A non-doped green device based on an ambipolar compound with a dibenzothiophene-*S*,*S*-dioxide core and two peripheral arylamines, also reported by Wu *et al.*[10], exhibited a current efficiency of 7.5 cd·A^{-1}, and the electron and hole mobilities of this compound are both about 10^{-4} $cm^2 \cdot V^{-1} \cdot s^{-1}$. However, there are few reports on non-doped red-emitting single-layer OLEDs based on small molecules until now and the performances are far behind the blue and green ones[5–10]. In 2004, Lin *et al.*[9] reported a few non-doped red-emitting single-layer OLEDs based on bipolar benzo [1,2,5] thiadiazole deriveatives, which exhibited a current efficiency of 0.5 cd·A^{-1}. One of the reasons for the poor performance in non-doped red-emitting single-layer OLEDs is that non-doped red electroluminescent (EL) materials are either with strong donor-acceptor (D-A) polar substituents[11–12] or with an extended π-conjugation[13–14]. Such materials tend to aggregate in highly concentrated solutions or solid states because of either dipole–dipole interaction or effective intermolecular $\pi-\pi$ stacking, which hence result in strong concentration quenching[15].

In our previous work[16], we have synthesized and characterized a novel red-emitting material: 4,9-bis(4-(2,2-diphenylvinyl) phenyl)naphtho[2,3-*c*][1,2,5]thiadiazole (BDPNTD) as shown in Fig.1. We demonstrated that a non-doped pure-red double-layer OLED with BDPNTD as the emitter showed a current efficiency of 2.05 cd·A^{-1} and a turn-on voltage of 2.8 V. In addition, it is worth noting that BDPNTD is an excellent ambipolar material with balanced electron and hole mobilities (both in the order of 10^{-4} $cm^2 \cdot V^{-1} \cdot s^{-1}$)[17], thus it is a promising candidate for the single-layer devices. The injection barrier between BDPNTD and the Mg:Ag cathode is very low (ca 0.12 eV). However, the injection barrier between BDPNTD and the ITO anode is a little large (ca 0.92 eV) as shown in Fig.2. Thus, modification of the anode in order to enchance the hole injection is a key issue for achieve non-doped single layer OLED based on BDPNTD.

1 Experimental

In this paper, to achieve a balance of electron and hole injection inside light-emitting layer, we inserted an ITO buffer layer, such as MoO_3[18], WO_3[19], and Au[20], between ITO and BDPNTD. The device configurations used in our experiments are: (i) ITO/WO_3 (1 nm)/BDPNTD (80 nm)/Mg:Ag (mass ratio of 10:1, 150 nm)/Ag (100 nm); (ii) ITO/MoO_3 (1 nm)/BDPNTD (80 nm)/Mg:Ag (mass ratio of 10:1, 150 nm)/Ag (100 nm); (iii) ITO/Au (5 nm)/BDPNTD (80 nm)/Mg:Ag (mass ratio of 10:1, 150 nm)/Ag (100 nm). The ITO coated glass substrate with a sheet resistance of 7 Ω·□$^{-1}$ was cleaned by O_2-plasma treatment. BDPNTD, MoO_3, WO_3 and Au films were fabricated by a conventional evaporation method. Mg:Ag (mass ratio of 10:1) layer covered by Ag was formed as cathode. Fig.2 shows energy level diagrams[18–20] of the devices. Voltage–current–luminance measurements were carried out with a Keithley 4200 and the EL spectra were recorded on a Photo Research PR705 spectrophotometer. All the devices were measured in air at room temperature without further encapsulation.

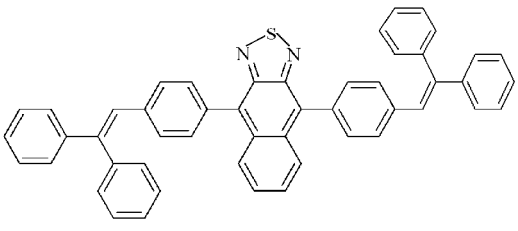

Fig.1 Molecular structure of BDPNTD

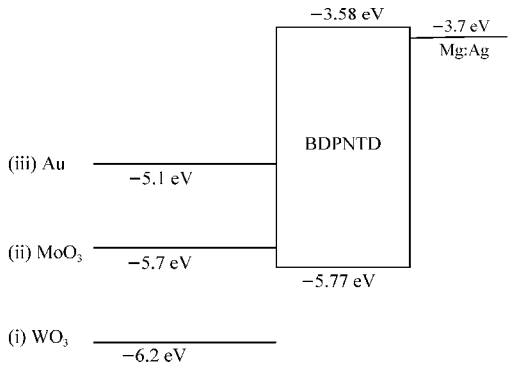

Fig.2 Energy level diagrams of the devices

(i) ITO/WO_3 (1 nm) /BDPNTD (80 nm)/Mg:Ag; (ii) ITO/MoO_3 (1 nm)/ BDPNTD (80 nm)/Mg:Ag; (iii) ITO/Au (5 nm)/BDPNTD (80 nm)/Mg:Ag

2 Results and discussion

Fig.3 shows the current density (*J*)–voltage (*V*)–brightness (*B*) characteristics of the devices and Table 1 summarizes the EL data of the non-doped single-layer OLEDs. As shown in Fig.4, the devices based on BDPNTD exhibit red emissions with the maximum emission wavelength at about 636 nm and the CIE coordinates around (0.65, 0.35). As shown in Table 1, the EL spectra exhibit little difference with different ITO buffer layers except the Au-modified anode device. Au layer (5 nm) has an absorption between 600 and 800 nm, as shown in Fig.5, leading to a blue shift in the light emission of device (iii). We also optimized the thicknesses of ITO buffer layers in the devices, and Table 2

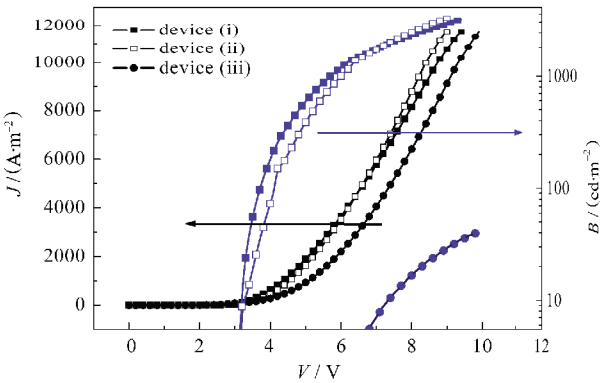

Fig.3 Current density (*J*)–voltage (*V*)–brightness (*B*) characteristics of the devices

(i) ITO/WO_3 (1 nm)/BDPNTD (80 nm)/Mg:Ag, (ii) ITO/MoO_3 (1 nm)/ BDPNTD (80 nm)/Mg:Ag, (iii) ITO/Au (5 nm)/BDPNTD (80 nm)/Mg:Ag

Table 1 EL data of the non-doped single-layer OLEDs with BDPNTD as the red-emitting material

Device	Materials	V_{on}/V	L_{max}/(cd·m^{-2}) (V(at L_{max})/V)	$\eta_{c,max}$/(cd·A^{-1})	$\lambda_{em,max}$/nm	CIE (x, y)
i	WO_3	2.4	4950 (15.0)	0.42	636	(0.64, 0.35)
ii	MoO_3	2.7	4740 (19.8)	0.41	636	(0.65, 0.35)
iii	Au	4.8	41 (10.1)	0.003	622	(0.63, 0.37)

V_{on}: turn-on voltage at the brightness of 1 cd·m^{-2}, L_{max}: the maximum luminance, V: voltage, $\eta_{c,max}$: the maximum current efficiency, $\lambda_{em,max}$: the maximum emission wavelength, CIE: Commission Internationale de L′Eclairage (CIE) 1931 coordinates

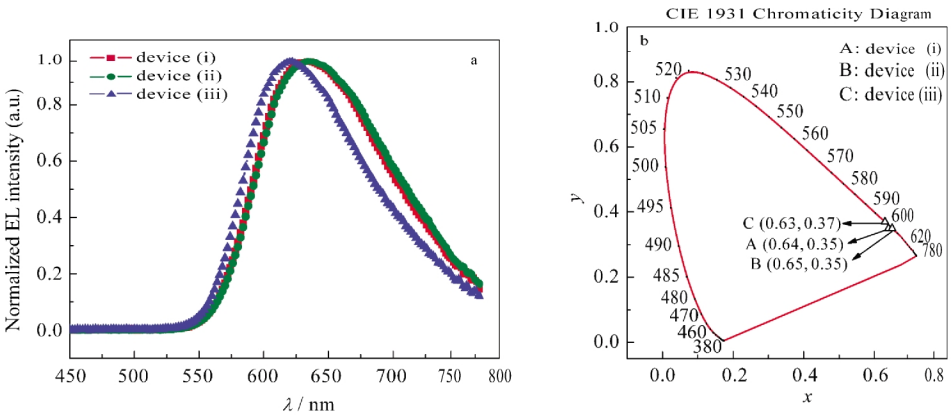

Fig.4 EL spectra (a) and CIE coordinates at 6 V (b) of the devices

Table 2 EL data of the non-doped single-layer OLEDs with different thicknesses of MoO_3

Device	Thickness of MoO_3 (nm)	V_{on}/V	L_{max}/(cd·m^{-2}) (V(at L_{max})/V)	$\eta_{c,max}$/(cd·A^{-1})	$\lambda_{em,max}$/nm	CIE (x, y)
ii-1	0.5	2.9	3591 (10.2)	0.31	636	(0.64, 0.36)
ii-2	1	2.7	4740 (9.8)	0.41	636	(0.65, 0.35)
ii-3	2	2.8	4112 (10.4)	0.35	636	(0.65, 0.35)
ii-4	5	2.7	3586 (10.3)	0.31	636	(0.65, 0.35)
ii-5	10	2.8	3354 (10.8)	0.29	636	(0.65, 0.35)

shows the EL data of non-doped single-layer OLEDs with different thicknesses of MoO_3. As the thickness of MoO_3 increases, the turn-on voltage and the EL spectra are almost constant; however, the maximum luminance and the maximum current efficiency show much difference. It is confirmed that 1 nm is the proper thickness of MoO_3 in this kind of OLEDs, which means the hole injection is increased with the thickness of the buffer in the thin range of 0.5−1.0 nm and decreased gradually in the range of 1.0−10.0 nm. Zhao *et al.*[21] explained this phenomenon by tunneling effect and pointed out that there was an optimal thickness of the buffer layer.

The maximum current efficiencies of devices (i), (ii), and (iii) are 0.42, 0.41, and 0.003 cd·A^{-1}, respectively; and the maximum luminances of devices (i), (ii), and (iii) are 4950, 4740, and 41 cd·m^{-2}, respectively. Moreover, devices (i) and (ii) also showed lower turn-on voltages compared with device (iii). Obviously, devices (i) and (ii) have better performance compared to device (iii). The performance of device (iii) is poor due to the relatively high hole injection barrier (ca 0.67 eV, Fig.2) at Au/BDPNTD interface, indicating that Au is not a good candidate for improving the hole injection into BDPNTD.

For device (i) with 1 nm WO_3 and device (ii) with 1 nm MoO_3, the efficiency of hole injection was improved and the drive voltage was lowered. WO_3 and MoO_3 are both metal oxides with

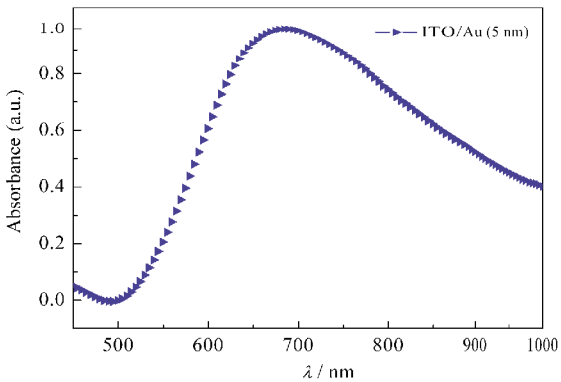

Fig.5 UV-Vis absorption spectrum of Au film (5 nm)

large work functions (WO_3 ca 6.2 eV[19] and MoO_3 ca 5.7 eV[18]). The hole injection barrier between ITO and BDPNTD is 0.92 eV. By inserting a thin MoO_3 film, the hole injection barrier is reduced to 0.07 eV. For WO_3, there is no hole injection barrier and Ohmic hole injection is achieved[22]. That is why device (i) with WO_3 shows the best performance among the three kinds of devices.

3 Conclusions

In summary, we designed three kinds of devices with an ambipolar molecule naphtho[2,3-*c*][1,2,5]thiadiazole derivative as

the nondoped emissive layer. MoO_3, WO_3, and Au have been employed as the ITO buffer layer. Non-doped single layer red light-emitting OLED was obtained with a luminance of 4950 $cd \cdot m^{-2}$ at 15.0 V, turn-on voltage of 2.4 V and the maximum current efficiency of 0.42 $cd \cdot A^{-1}$.

References

1 Tang, C. W.; VanSlyke, S. A. *Appl. Phys. Lett.*, **1987, 51**: 913

2 Hung, L. S.; Chen, C. H. *Mater. Sci. Eng. R-Rep.*, **2002, 39**: 143

3 Shirota, Y. *J. Mater. Chem.*, **2000, 10**: 1

4 Emi, H.; Toru, K.; Masaki, M. *Dyes Pigment.*, **2006, 70**: 43

5 Li, Z. H.; Wong, M. S.; Fukutani, H.; Tao, Y. *Org. Lett.*, **2006, 8**: 4271

6 Zhang, H. Y.; Huo, C.; Zhang, J. Y.; Zhang, P.; Tian, W. J.; Wang, Y. *Chem. Commun.*, **2006**: 281

7 Lai, M. Y.; Chen, C. H.; Huang, W. S.; Lin, J. T.; Ke, T. H.; Chen, L. Y.; Tsai, M. H.; Wu, C. C. *Angew. Chem. Int. Edit.*, **2008, 47**: 581

8 Liao, Y. L.; Lin, C. Y.; Wong, K. T.; Hou, T. H.; Hung, W. Y. *Org. Lett.*, **2007, 9**: 4511

9 Thomas, J. K. R.; Velusamy, M.; Lin, J. T.; Tao, Y. T.; Cheun, C. H. *Adv. Funct. Mater.*, **2004, 14**: 387

10 Huang, T. H.; Lin, J. T.; Chen, L. Y.; Lin, Y. T.; Wu, C. C. *Adv. Mater.*, **2006, 18**: 602

11 Tang, C. W.; VanSlyke, S. A.; Chen, C. H. *J. Appl. Phys.*, **1989, 65**: 3610

12 Chen, C. H.; Tang, C. W.; Shi, J.; Klubek, K. P. *Thin Solid Films*, **2000, 363**: 327

13 Burrows, P. E.; Forrest, S. R.; Sibley, S. P.; Thompson, M. E. *Appl. Phys. Lett.*, **1996, 69**: 2959

14 Sakakibara, Y.; Okutsu, S.; Enokida, T.; Tani, T. *Appl. Phys. Lett.*, **1999, 74**: 2587

15 Chen, C. T. *Chem. Mater.*, **2004, 16**: 4389

16 Qiu, Y.; Wei, P.; Zhang, D. Q.; Qiao, J.; Duan, L.; Li, Y. K.; Gao, Y. D.; Wang, L. D. *Adv. Mater.*, **2006, 18**: 1607

17 Wei, P.; Duan, L.; Zhang, D. Q.; Qiao, J.; Wang, L. D.; Wang, R. J.; Dong G. F.; Qiu, Y. *J. Mater. Chem.*, **2008, 18**: 806

18 Matsushima, T.; Kinoshita, Y.; Murata, H. *Appl. Phys. Lett.*, **2007, 91**: 253504

19 Son, M. J.; Kim, S.; Kwon, S.; Kim, J. W. *Org. Electron.*, **2009, 10**: 637

20 Fong, H. H.; Alexis, P.; Hwang, J.; Kahn, A.; Malliaras, G. G. *Adv. Funct. Mater.*, **2009**, **19**: 304

21 Zhao, J. M.; Zhang, S. T.; Wang, X. J.; Zhan, Y. Q.; Wang, X. Z.; Zhong, G. Y.; Wang, Z. J.; Ding, X. M.; Huang, W.; Hou, X. Y. *Appl. Phys. Lett.*, **2004, 84**: 2913

22 Yi, Y. J.; Jeon, P. E.; Lee, H.; Lan, K.; Kim, H. S.; Jeong, K.; Cho, S. W. *J. Chem. Phys.*, **2009, 130**: 094704